Korean J. Chem. Eng., 35(6), 1373-1379 (2018)
DOI: 10.1007/s11814-018-0023-y

pISSN: 0256-1115
eISSN: 1975-7220

Two dimensional Zn-stilbenedicarboxylic acid (SDC) metal-organic frameworks for cyclic carbonate synthesis from CO_2 and epoxides

Gak-Gyu Choi, Jintu Francis Kurisingal, Yongchul G. Chung†, and Dae-Won Park†

Division of Chemical and Biomolecular Engineering, Pusan National University, Busan 46241, Korea
(*Received 14 November 2017 • accepted 5 February 2018*)

Abstract−A two-dimensional Zn-based metal-organic framework has been synthesized by using Zn(II) ions and H_2SDC (4,4′-stilbenedicarboxylic acid) under solvothermal conditions. The framework having a trinuclear Zn_3-$(RCO_2)_6$ SBUs connected by the 4,4′-stilbenedicarboxylic acid to form a hexagonal network, shows a two-dimensional structure and displays high thermal stability up to approximately 330 °C. The role of Zn^{2+} (from Zn-SDC) for epoxide activation and Br^- ion (from TBABr) for ring opening of epoxide was studied for the cycloaddition reaction of CO_2 and propylene oxide (PO) under ambient conditions. Zn-SDC was found catalytically efficient towards CO_2-epoxide coupling under ambient reaction conditions with high selectivity towards the desired cyclic carbonates under solvent-free conditions. The effects of various reaction parameters such as catalyst loading, temperature, CO_2 pressure, and time were evaluated. Zn-SDC was easily separable and reusable at least five times without any considerable loss in the initial activity. A plausible reaction mechanism for the cycloaddition reaction was also proposed based on literature and experimental inferences.

Keywords: Metal Organic Frameworks, Zn-SDC, CO_2, Epoxide, Cyclic Carbonate

INTRODUCTION

Increasing concerns over Earth's atmospheric temperature (global warming) have prompted researchers to develop technologies to reduce the carbon dioxide emissions [1-3]. Many different technologies, such as post-/pre-combustion and atmospheric CO_2 capture, have been proposed to mitigate the accumulation of CO_2 in the atmosphere. The captured CO_2 can be compressed to 100 bar and transported to geological sequestration site for near-permanent sequestration. Alternatively, the captured CO_2 can be turned into a series of useful commodity chemicals which have industrial value, such as cyclic carbonates, dimethyl carbonate, formic acid, and urethanes. The five-membered cyclic carbonates are non-toxic solvents that can be prepared by catalytic conversion of carbon dioxide and epoxides, and can be used as a monomer precursor for the synthesis of polycarbonate copolymers, the coordination of lithium ions in solid polymer batteries, and as intermediates in the synthesis of pharmaceuticals [4-7].

Metal-organic frameworks (MOFs) are a class of inorganic-organic hybrid materials conventionally synthesized through solvothermal routes by linking secondary building units (SBUs) with organic spacers, resulting in diverse networks. MOFs are a new and emerging class of porous material that possesses interesting characteristics such as high micropore volume, confined pore size with high crystallinity, and a high metal content to achieve active sites [8-11]. MOFs are widely studied because of their potential applications in many areas such as luminescence, magnetism, drug storage and delivery, gas storage, adsorption and separation, and catalysis. To date, more than 6,000 MOFs have been synthesized and reported in the literature [12], and a variety of MOF synthetic methods including hydro/solvothermal [13], microwave-assisted [14,15], sonochemical [16] and mechanochemical [17] routines have been developed for the synthesis of MOF catalysts.

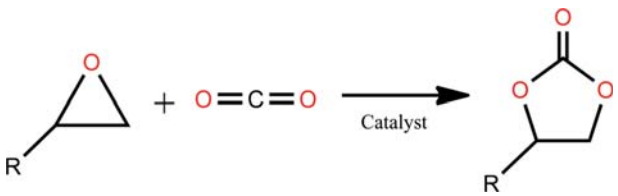

Scheme 1. Synthesis of cyclic carbonate using PO and CO_2.

Due to the presence of active sites in some MOFs, MOFs can be used as efficient catalyst materials for epoxide-CO_2 cycloadditions (Scheme 1). There have been many investigations which describe the catalytic activity of MOFs for the synthesis of various cyclic carbonates under mild conditions in the presence of various quaternary ammonium salts [18,19]. Recently, different transition-metal-based porous carboxylate (such as benzene dicarboxylate, benzene tricarboxylate, naphthalene dicarboxylate) MOFs with high CO_2 adsorption capacity have been reported for epoxide-CO_2 cycloaddition reactions. In this work we focused on stilbene-based two-dimensional Zn-based MOF (Zn-SDC). Zn-SDC is demonstrated as the first example of 4,4-stilbenedicaroxylic acid based MOF catalyst that participates in the cycloaddition of epoxides and CO_2. Moreover, two dimensional MOFs have been rarely reported for the synthesis of cyclic carbonates. Herein, we report the catalytic potential of two-dimensional Zn-SDC [20] in the coupling

†To whom correspondence should be addressed.
E-mail: dwpark@pusan.ac.kr, greg.chung@pusan.ac.kr

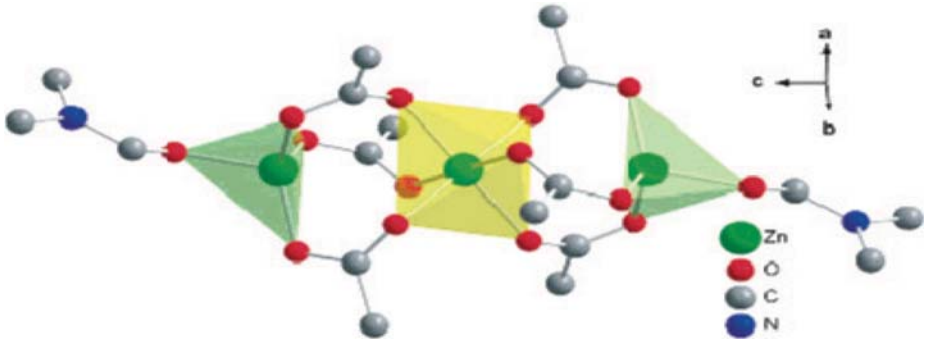

Fig. 1. Pictorial representation of the Zn-SDC metal organic framework with Zn as the metal centers surrounded by the organic ligand.

reaction of CO_2 with epoxides to yield five-membered cyclic carbonates. Our results show that the material can act as an efficient catalyst for different cycloaddition reactions.

EXPERIMENTAL

1. Chemicals

$Zn(NO_3)_2{\cdot}6H_2O$ (Sigma Aldrich), 4,4′-stilbenedicarboxylic acid (TCI), acetic acid (Alfa Aesar), N,N-dimethylformamide (TCI), dichloromethane (Sigma Aldrich) chloroform (Sigma-Aldrich), toluene (sigma-Aldrich), propylene oxide (Sigma-Aldrich), and tetrabutylammonium bromide (TBABr, Sigma Aldrich) were used as received without further treatment.

2. Synthesis of Zn-SDC

For the preparation of Zn-SDC [25], 0.63 g of $Zn(NO_3)_2{\cdot}6H_2O$ was dissolved in 30 mL N,N-dimethylformamide and stirred for 5 min. Subsequently, 0.21 g of 4,4′-stilbenedicarboxylic acid was dissolved in another 30 mL N,N′-dimethylformamide and then mixed with the above metal solution and again stirred for 5 min. The mixed solution was poured into 100 mL Teflon lined autoclave and left at a temperature of 85 °C for 24 h in the oven. The reaction mixture was allowed to cool to room temperature, and the crystals produced were washed with chloroform three times, centrifuged, and then dried in a vacuum oven at 60 °C.

3. Carbon Dioxide-epoxide Cycloaddition Reactions

Cycloaddition reactions were carried out in a 25 mL stainless steel reactor equipped with a magnetic stirrer. Procedure for the synthesis of cyclic carbonate from epoxide was as follows. An appropriate amount of activated, finely ground catalyst was added to the reactor containing 42.9 mmol of epoxide. The reactor was pressurized with CO_2 to the required pressure at room temperature, brought to the desired temperature, and stirred at 500 rpm. In a typical semi-batch operation, a back-pressure regulator was installed to maintained reactor pressure constant. Therefore, CO_2 was supplied automatically as soon as it was consumed by the reaction. After reaction completion, the reactor was cooled to 5 °C and excess CO_2 was carefully vented off. 3 mL of toluene was added to the product mixture as internal standard and centrifuged. The supernatant was subsequently analyzed using gas chromatography (Agilent HP 6890A) equipped with a capillary column (HP-5, 30 m×0.25 μm) using a flame ionization detector to determine conversion, selectivity, and yield.

RESULTS AND DISCUSSION

1. Characterizations of Catalysts

Zn-SDC is a crystalline material having the molecular formula of $C_{34}H_{44}N_2O_{14}Zn_3$ with a two-dimensional structure consisting of zinc metal in both octahedral and tetrahedral environments linked by 4,4′-stilbenedicarboxylic acid. A framework having a trinuclear Zn_3-$(RCO_2)_6$ SBUs was connected by the organic linker to form a hexagonal network. Fig. 1 shows Zn_3-$(RCO_2)_6$ SBUs lying on a 3-fold axis, containing a linear arrangement of zinc atoms, in which the central and terminal metal site (Zn atom) were coordinated octahedrally and tetrahedrally. The central zinc atom has longer Zn-O bonds (2.1 Å) than those of the terminal Zn-O bonds (1.9 Å). The Zn_3-$(RCO_2)_6$ SBUs are connected with stilbene units in a hexagonal pinwheel geometry having a two-dimensional structure and filling space above and below the layer by disordered DMF units [20].

To confirm the crystallinity, phase homogeneity, and phase purity of the synthesized sample, the PXRD pattern of Zn-SDC was compared with its simulated pattern from single crystal data. All the obtained peaks matched perfectly with those of the simulated PXRD pattern (Fig. 2). The FT-IR spectra of Zn-SDC are shown in Fig. 3. The band at 1,734 cm^{-1} corresponds to the C=O stretching vibration, and the peaks at around 1,455 cm^{-1} are attributed to the C-H

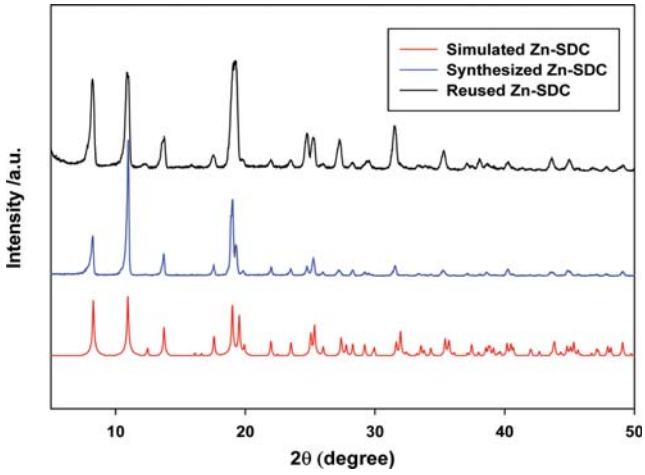

Fig. 2. PXRD patterns of Zn-SDC (synthesized, simulated and reused).

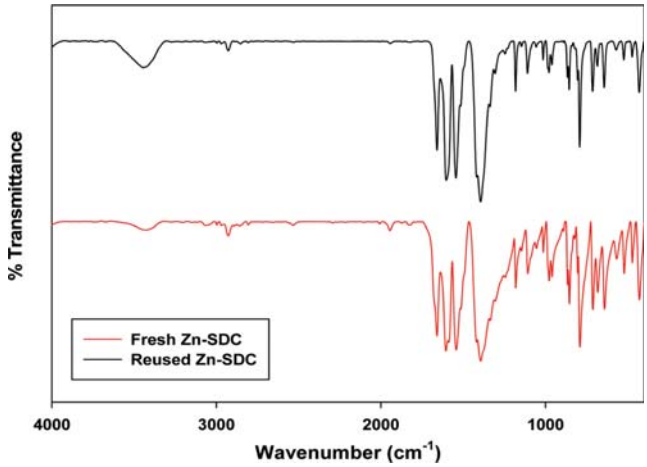

Fig. 3. FT-IR spectra of fresh Zn-SDC and reused Zn-SDC.

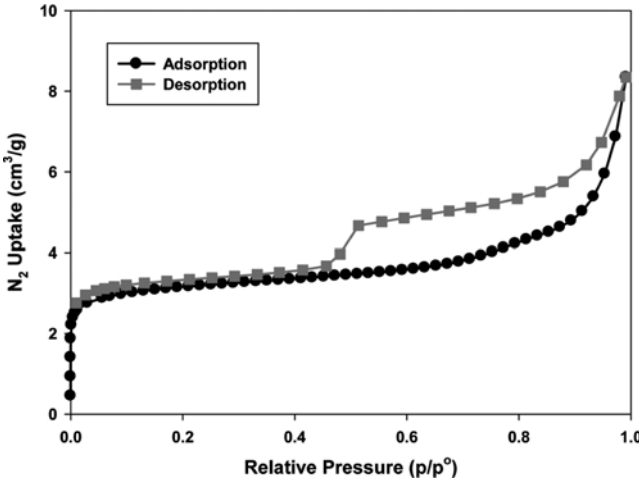

Fig. 5. N_2 adsorption and desorption for Zn-SDC at −195 °C.

bending vibration. The peaks at around 1,555 and 763 cm^{-1} correspond to C=C stretching and bending vibrations, respectively. The presence of a Zn-O bond peak at 492 cm^{-1} indicates the successful formation of the Zn-SDC. The FE-SEM image of the Zn-SDC shown in Fig. S1 reveals the formation of well-defined crystal particles. The crystal faces of Zn-SDC have uniform plate-like morphology.

Elemental analysis (EA) and inductively coupled plasma atomic emission spectrophotometer (ICP-OES) of the prepared Zn-SDC was almost similar to the calculated value as shown in Table S1. Zn content in the synthesized Zn-SDC was 16.65 wt%. The thermogravimetric analysis (TGA) shown in Fig. 4 displays the thermal stability of the synthesized Zn-SDC. A small weight loss up to 300 °C corresponding to the loss of coordinated DMF was observed, followed by a major weight loss over 350 °C, indicating that the material is thermally stable up to 350 °C. XPS analyses were performed to confirm the states of Zn in the catalyst system. As shown in Fig. S2 and definitive peak at 1,022.8 eV for the Zn 2p^3 was found. CO_2 and NH_3 TPD were performed on Zn-SDC to evaluate the acid-base characteristics in the catalytic system (Fig. S3). The amount of acid and base sites was 1.12 and 0.22 mmol/g, respectively. BET analysis of nitrogen adsorption at −195 °C for Zn-SDC in shown in Fig. 5. Zn-SDC exhibits very small BET surface area (11.9 m^2/g) as expected due to its high density and the pore occlusion evident in their crystal structure. CO_2 adsorption capacity was also tested at 25 °C. Fig. S4 shows the adsorbed amount of CO_2 by Zn-SDC. The adsorption/desorption profile displays hysteresis, suggesting that there may also be a structural alteration due to the interaction between the catenated units and/or linkers.

2. Cycloaddition Reactions

Propylene oxide (PO) was used as the model substrate to evaluate the catalytic activity of Zn-SDC. As shown in Table 1, no significant conversion of PO occurred at 60 °C, 1.2 MPa, in 6 h under catalyst-free conditions (Entry 1). However, a slight increase in the PC yield was observed when only TBABr (co-catalyst) was used under the same reaction conditions (Entry 2). A set of experiments was conducted with the precursors of the Zn-SDC and TBABr (Table 1, Entries 3 and 4). Precursors of Zn-SDC displayed higher

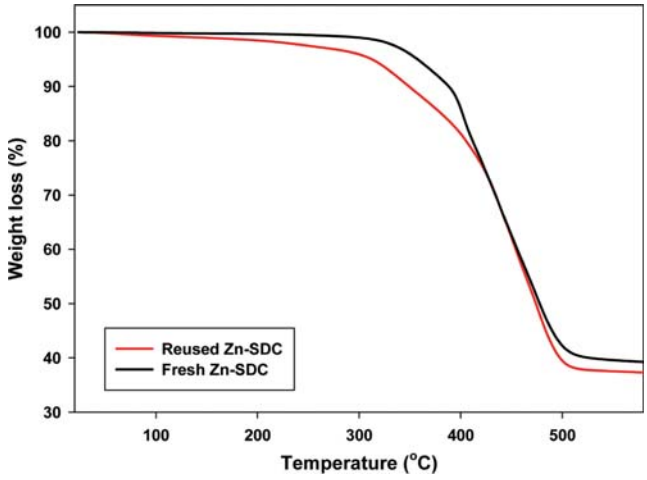

Fig. 4. Thermal gravimetric analysis (TGA) of fresh and reused Zn-SDC.

Table 1. Performance of Zn-SDC in the cycloaddition of CO_2 with propylene oxide (PO)

Entry	Catalyst	Conversion (%)	Selectivity (%)
1	None	-	-
2	TBABr	11	>99
3	SDC/TBABr	45	98
4	$Zn(NO_3)_2{\cdot}6H_2O$/TBABr	22	95
5	$Zn(NO_3)_2{\cdot}6H_2O$/SDC/TBABr	64	92
6	Zn-SDC	>5	>99
7	Zn-SDC/TBABr	94	>99
8	Zn-SDC/TBACl	55	>99
9	Zn-SDC/TBAI	33	>99

Reaction Conditions: Propylene oxide (PO)=42.8 mmol, Catalyst=0.8 mol%, TBABr=0.8 mol%, P=1.2 MPa CO_2, T=60 °C, t=6 h, semi batch reaction

PO conversion than that of TBABr alone. Combination of the metal salt ($Zn(NO_3)_2{\cdot}6H_2O$), the linker (SDC), and TBABr afforded 64% conversion under the same reaction conditions (entry 5). Zn-SDC/TBABr system exhibited an excellent PO conversion of 94% with >99% selectivity towards PC (Table 1, Entry 7). The effect of the halide ions in the tetraalkyl ammonium salt (using TBAI and TBACl co-catalysts) towards the cycloaddition reactions was also conducted, and the results are given in Table 1, entries 8 and 9. The highest activity was obtained with Br^- followed by Cl^- (55%), and then I^- (33%). Even though I^- is the most nucleophilic anion among the three anions, it showed the lowest PO conversion due to the steric hindrance.

Various reaction parameters such as the amount of catalyst, temperature, time, and CO_2 pressure for the Zn-SDC-mediated PO-CO_2 cycloaddition were investigated for the optimization of reaction conditions. The effect of Zn-SDC catalyst amount on the cyclic carbonate synthesis under the reaction conditions of 1.2 MPa of CO_2 for 6 h at 60 °C was studied and displayed in Fig. 6. The PO conversion was increased linearly with the increase in Zn-SDC amount ranging from 0.2 mol% to 1 mol%, with >99% selectivity of PC. A maximum PO conversion of 94% with >99% PC selectivity was observed for Zn-SDC at 0.8 mol% of catalyst amount under the reaction conditions. Fig. 7 depicts the effect of the reaction time on the Zn-SDC catalyzed cycloaddition reaction ranging from 2 to 10 h with 0.8 mol% catalyst, 1.2 MPa CO_2 pressure at 60 °C. The PO conversion increased with reaction time and approached almost 100% conversion at 10 h.

The effects of the temperature on the catalytic activities of Zn-SDC under the reaction conditions of 1.2 MPa of CO_2 pressure for 6 h, are shown in Fig. 8. A steady incremental increase in PO conversion with an increase in temperature from RT to 80 °C ranges was observed, reaching its best conversion at a temperature of 60 °C and then remaining constant until 80 °C. A study of the effect of the CO_2 pressure on the catalysis of the cycloaddition reaction was conducted in the range of 0.3-1.8 MPa with catalyst amount

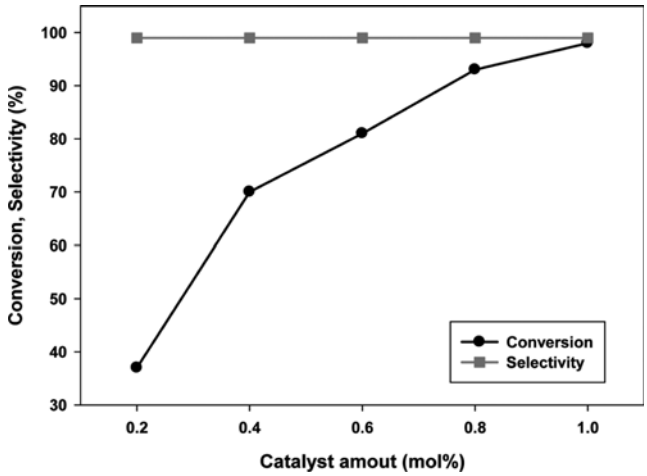

Fig. 6. Effect of catalyst amount of Zn-SDC on the cycloaddition of PO and CO_2 (Reaction condition: PO=42.8 mmol, T=60 °C, t=6 h, P_{CO_2}=1.2 MPa).

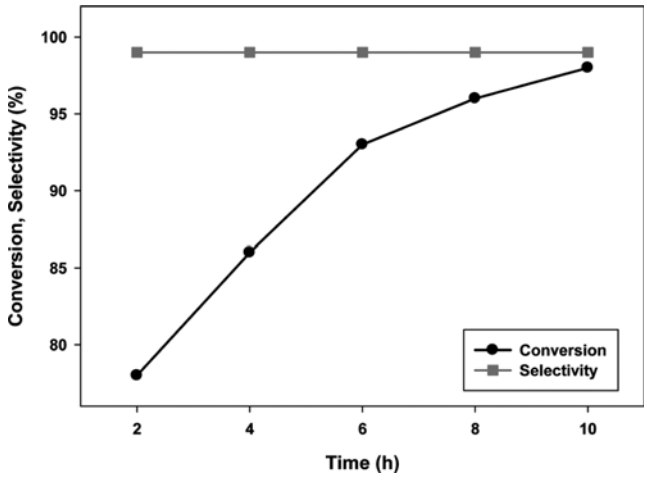

Fig. 7. Influence of reaction time on the cycloaddition of PO and CO_2 (Reaction condition: PO=42.8 mmol, Zn-SDC=0.8 mol%, TBABr=0.8 mol%, T=60 °C, P_{CO_2}=1.2 MPa).

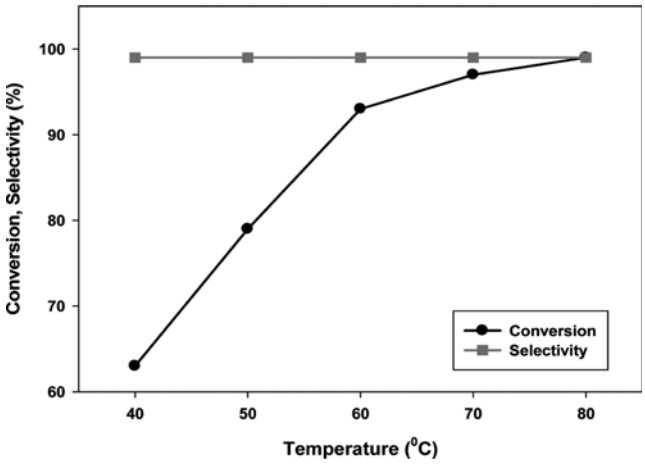

Fig. 8. Influence of reaction temperature on the cycloaddition of PO and CO_2 (Reaction condition: PO=42.8 mmol, Zn-SDC= 0.8 mol%, TBABr=0.8 mol%, t=6 h, P_{CO_2}=1.2 MPa).

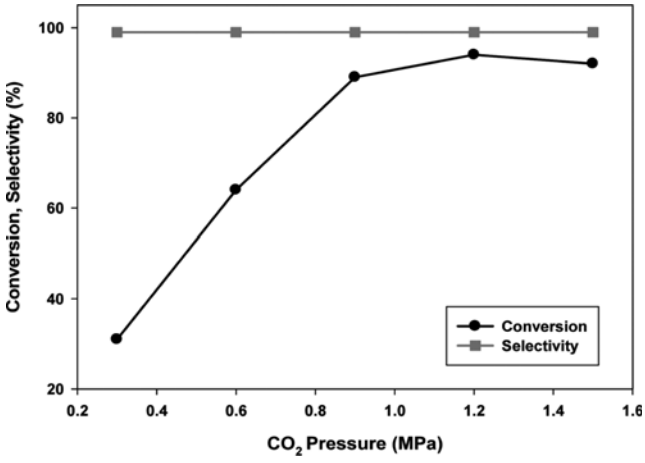

Fig. 9. Effect of pressure on the cycloaddition of PO and CO_2 (Reaction condition: PO=42.8 mmol, Zn-SDC=0.8 mol%, TBABr= 0.8 mol%, T=60 °C, t=6 h).

Table 2. Synthesis of cyclic carbonates from other epoxides

Entry	Reactant	Conversion (%)	Selectivity (%)	Yield (%)
1	Propylene oxide	94	>99	94
2	Epichlorohydrin	82	>99	82
3	Allyl glycidyl ether	67	>99	67
4	Styrene oxide	44	>99	44
5	Cyclohexene oxide	14	>99	14
6	1,2-Epoxyoctane	58	>99	58

Reaction conditions: Epoxide (42.8 mmol), Zn-SDC (0.8 mol%), TBABr (0.8 mol%), P=1.2 MPa CO_2, T=60 °C, t=6 h, semi-batch operation

of 0.8 mol% at 60 °C for 6 h, and is depicted in Fig. 9. PO conversion increases steeply with an increase in CO_2 pressure from 0.3 to 1.2 MPa and reaches a maximum PO conversion of 94%, then it decreases slightly at 1.6 MPa. According to previous study, it could be explained that PO was in its liquid state under the reaction conditions. At low-pressure region, the concentration of CO_2 in the liquid state rose with increasing pressure, which promoted the reaction. But high CO_2 pressure (1.6 MPa) would slightly decrease the PC yield because of the lower concentration of PO in the liquid state, since PO is also a reactant [21,22].

The scope of Zn-SDC-mediated epoxide-CO_2 coupling reaction was extending towards different epoxides under the optimized reaction conditions; the results are shown in Table 2. Terminal epoxides such as epichlorohydrin, allyl glycidyl ether gave comparatively better activity towards cyclic carbonates (Entry 2 and 3) [23-25]. The aromatic epoxide styrene oxide exhibits comparatively lower conversion over Zn-SDC but with >99% selectivity (Entry 4). Meanwhile, the internal epoxide cyclohexane oxide gave very low conversions (Entry 5), which could be ascribed to the steric effect of the cyclohexene ring. Notably long chain epoxide, 1,2-epoxyoctane exhibits 58% conversion with >99% selectivity (entry 6).

Some reported MOFs have difficulties in reusability in the coupling reaction of epoxide and CO_2 mainly due to the loss of active site or pore blocking, structural disorder etc. We performed reusability studies of Zn-SDC using the reaction of PO and CO_2 under the optimized reaction conditions. We found that PO conversion and PC selectivity was preserved throughout the five cycles, showing the stability and efficiency of the catalyst system (Fig. 10). The major characteristic peaks of PXRD of the recycled Zn-SDC were similar to those of the fresh catalyst, showing that structural integrity of material was maintained throughout the process (Fig. 2). Chemical integrity of Zn-SDC remained intact after being recycled five times, which was determined by FT-IR analysis (Fig. 3). The TGA pattern of recycled Zn-SDC showed the stability of the material as shown in (Fig. 4). ICP-OES analysis of the recycled Zn-SDC revealed that less than 0.5% of Zn was leached from the catalysts after the five successive recycle process.

Having identified the catalytic potential of Zn-SDC to materialize the synthesis of five membered cyclic carbonates, we compared the catalytic activity of Zn-SDC with aluminum containing MOF having the same linker SDC. We synthesized Al-SDC [26] and

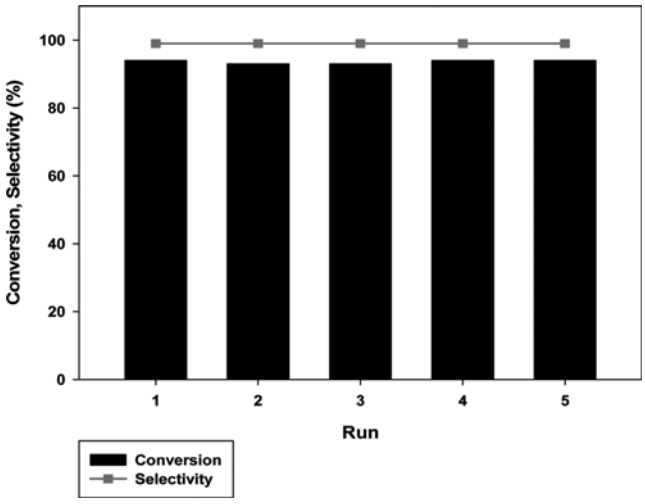

Fig. 10. Reusability performance of Zn-SDC catalyst (Reaction conditions: PO=42.8 mmol, Zn-SDC=0.8 mol% TBABr=0.8 mol%, t=6 h, T=60 °C, P_{CO_2}=1.2 MPa).

attempted a comparison at the same reaction conditions of Zn-SDC. Zn-SDC containing a linear arrangement of zinc atoms has two different metal sites: the central and terminal metal site (Zn atom) coordinated octahedrally and tetrahedrally, respectively. With the advantages of tetrahedrally coordinated terminal Zn atom (unsaturated), the Zn-SDC afforded an excellent 94% PO conversion with >99% selectivity towards PC. Zn-SDC has a structure with fully coordinated and uncoordinated Zn^{2+} metal center, and the unsaturated site acts as good site for epoxide activation. Meanwhile, fully coordinated Al center in the Al-SDC exhibited only 35% PO conversion with >99% PC selectivity at the same optimized reaction condition of Zn-SDC. It shows that fully coordinated metal center is less effective in the epoxide activation in the synthesis of cyclic carbonates.

3. Mechanism

A plausible reaction mechanism of the cycloaddition reaction catalyzed by Zn-SDC in the presence of TBABr as co-catalyst is illustrated in Scheme 2. Initially, the epoxide oxygen is activated by the Lewis acidic Zn(II) center of Zn-SDC. Subsequently, the anion Br^- of co-catalyst attacks the least hindered carbon atom, which opens up the PO ring. Then, the O^- of the ring opened intermediate structure attacks the carbon atom of CO_2, forming a carbonate complex, as has been proposed in other literatures [27-31]. In the following step, ring closure happens by intramolecular carbonate O^- attack on the C-Br carbon where the cyclic carbonate (PC) is synthesized and liberated from the catalyst and co-catalyst.

CONCLUSIONS

We report the catalytic properties of zinc-based metal organic framework with 4,4′-stilbenedicarboxylic acid as ligand (Zn-SDC) for the synthesis of five-membered cyclic carbonates in a solvent-free medium. We observed 94% and 99% of conversion of PO and selectivity of PC, respectively, under optimized reaction conditions in the presence of the co-catalyst TBABr. The reusability test of Zn-SDC showed that the catalyst retains its performance even after

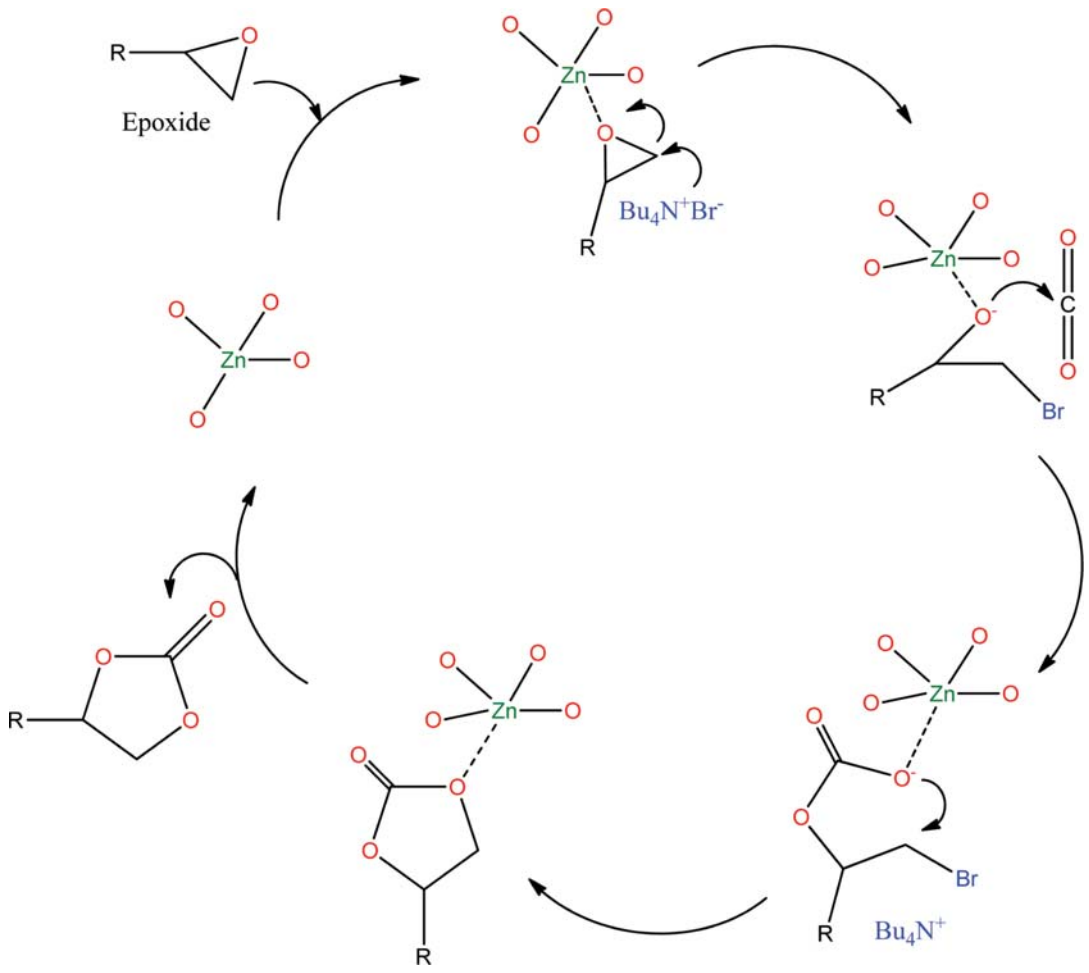

Scheme 2. Possible mechanism for the Zn-SDC catalyzed cycloaddition of PO and CO_2.

undergoing the reactions more than five times under the reaction conditions that we investigated.

ACKNOWLEDGEMENTS

This work was supported by a 2-year Research Grant of Pusan National University to Yongchul G. Chung.

SUPPORTING INFORMATION

Additional information as noted in the text. This information is available via the Internet at http://www.springer.com/chemistry/journal/11814.

REFERENCES

1. S. Klaus, M. W. Lehenmeier, C. E. Anderson and B. Rieger, *Coord. Chem. Rev.*, **255**, 1460 (2011).
2. M. Aresta and A. Dibenedetto, *Dalton Trans.*, **28**, 2975 (2007).
3. J. Melendez, M. North and P. Villuendas, *Chem. Commun.*, **18**, 2577 (2009).
4. M. Tu and R. J. Davis, *J. Catal.*, **199**, 85 (2001).
5. E. J. Doskocil, *Micropor. Mesopor. Mater.*, **76**, 177 (2004).
6. E. J. Doskocil, *J. Phys. Chem. B.*, **109**, 2315 (2005).
7. R. Srivastava, D. Srinivas and P. Ratnasamy, *Appl. Catal. A: Gen.*, **289**, 128 (2005).
8. D. Alhashmialameer, J. Collins, K. Hattenhauera and F. M. Kerton, *Catal. Sci. Technol.*, **6**, 5364 (2016).
9. D. J. Darensbourg and S. B. Fitch, *Inorg. Chem.*, **47**, 11868 (2008).
10. P. P. Pescarmona and M. Taherimehr, *Catal. Sci. Technol.*, **2**, 2169 (2012).
11. S. N. Kim, J. Kim, H. Y. Kim, H. Y. Cho and W. S. Ahn, *Catal. Today*, **204**, 85 (2013).
12. Y. G. Chung, J. Camp, M. Haranczyk, B. J. Sikora, W. Bury, V. Krungleviciute, T. Yildirim, O. K. Farha, D. S. Sholl and R. Q. Snurr, *Chem. Mater.*, **26**, 21 (2014).
13. R. Babu, A. C. Kathalikkattil, R. Roshan, J. Tharun, D. W. Kim and D. W. Park, *Green Chem.*, **18**, 232 (2016).
14. R. Babu, R. Roshan, A. C. Kathalikkattil, D. W. Kim and D. W. Park, *ACS Appl. Mater. Interfaces*, **8**, 33723 (2016).
15. A. C. Kathalikkattil, D. W. Kim, J. Tharun, H.-G. Soek, R. Roshan and D. W. Park, *Green Chem.*, **16**, 1607 (2014).
16. W. J. Son, J. Kim, J. Kim and W. S. Ahn, *Chem. Commun.*, **47**, 6336 (2008).
17. Y. Chen, J. Xiao, D. Lv, T. Huang, F. Xu, X. Sun, H. Xi, Q. Xia and Z. Li, *Chem. Eng. Sci.*, **158**, 539 (2017).

18. J. Tharun, G. Mathai, A. C. Kathalikkattil, R. Roshan, Y. S. Won, S. J. Cho, J. S. Chang and D. W. Park, *ChemPlusChem*, **80**, 715 (2015).
19. R. Babu, A. C. Kathalikkattil, R. Roshan, J. Tharun, D. W. Kim and D. W. Park, *Green Chem*., **18**, 232 (2016).
20. C. A. Bauer, T. V. Timofeeva, T. B. Settersten, B. D. Patterson, V. H. Liu, B. A. Simmons and M. D. Allendorf, *J. Am. Chem. Soc*., **129**, 7136 (2007).
21. Y. Xie, Z. Zhang, T. Jiang, J. He, B. Han, T. Wu and K. Ding, *Angew. Chem. Int. Ed*., **46**, 7255 (2007).
22. P. B. Webb, M. F. Sellin, T. E. Kunene, S. Williamson, A. M. Z. Slawin and D. J. Cole-Hamilton, *J. Am. Chem. Soc*., **125**, 15577 (2003).
23. K. R. Roshan, G. Mathai, J. Kim, J. Tharun, G. A. Park and D. W. Park, *Green Chem*., **14**, 2933 (2012).
24. G. W. Coates and D. R. Moore, *Angew. Chem. Int. Ed*., **43**, 6618 (2004).
25. J. J. Peng and Y. Deng, *New J. Chem*., **25**, 639 (2001).
26. S. H. Lo, C. H. Chien, Y. L. Lai, C. C. Yang, J. J. Lee, D. S. Raja and C. H. Lin, *J. Mater. Chem. A*., **1**, 324 (2013).
27. D. J. Darensbourg and S. B. Fitch, *Inorg. Chem*., **47**, 11868 (2008).
28. P. P. Pescarmona and M. Taherimehr, *Catal. Sci. Technol*., **2**, 2169 (2012).
29. T. Lescouet, C. Chizallet and D. Farrusseng, *ChemCatChem*, **4**, 1725 (2012).
30. S. N. Kim, J. Kim, H. Y. Kim, H. Y. Cho and W. S. Ahn, *Catal. Today*, **204**, 85 (2013).
31. J. Tharun, G. Mathai, A. C. Kathalikkattil, R. Roshan, Y. S. Won, S. J. Cho, J. S. Chang and D. W. Park, *ChemPlusChem*, **80**, 715 (2015).

Supporting Information

Two dimensional Zn-stilbenedicarboxylic acid (SDC) metal-organic frameworks for cyclic carbonate synthesis from CO_2 and epoxides

Gak-Gyu Choi, Jintu Francis Kurisingal, Yongchul G. Chung†, and Dae-Won Park†

Division of Chemical and Biomolecular Engineering, Pusan National University, Busan 46241, Korea
(*Received 14 November 2017 • accepted 5 February 2018*)

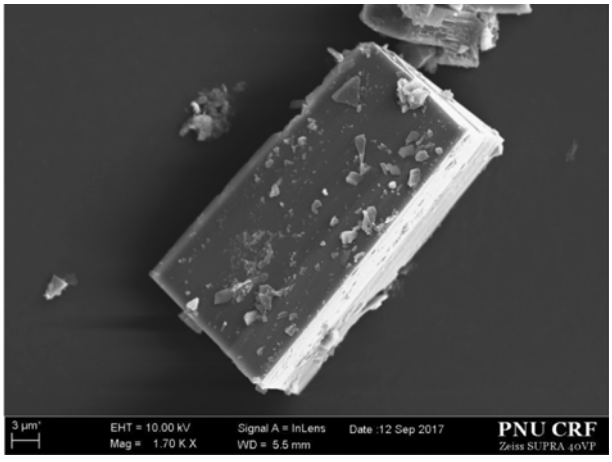

Fig. S1. FE-SEM images of Zn-SDC.

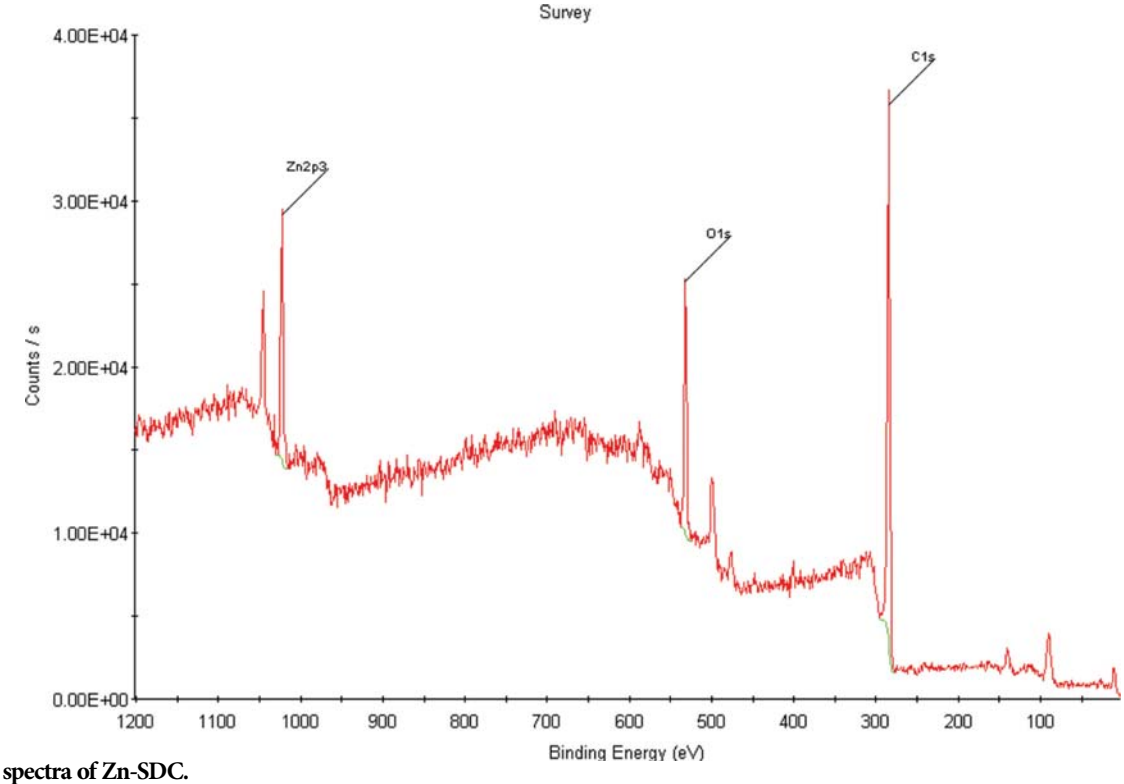

Fig. S2. XPS spectra of Zn-SDC.

(a)

No.	Start time (sec)	End time (sec)	Time width (sec)	Peak position (sec)	Peak position (℃)	Area (count)	mmol	mmol/g	log(W/F)+3
1	3769	5826	2058	4586	112.7	416,975	0.015	0.308	
2	5827	7639	1813	6617	270.5	1,096,385	0.041	0.811	

(b)

No.	Start time (sec)	End time (sec)	Time width (sec)	Peak position (sec)	Peak position (℃)	Area (count)	mmol	mmol/g	log(W/F)+3
1	3739	5838	2100	5219	160.2	64,116	0.001	0.029	
2	5839	7637	1799	6598	260.7	413,346	0.008	0.188	

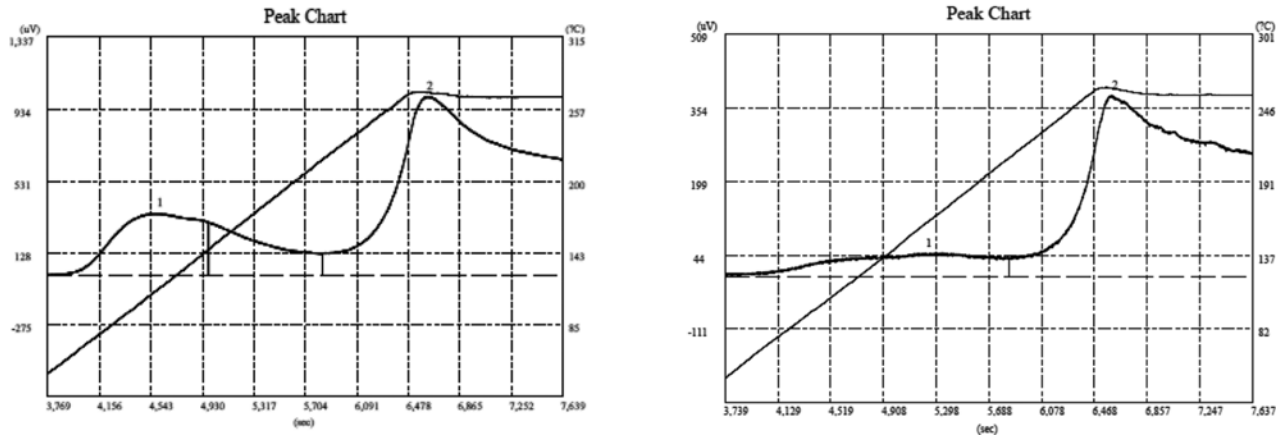

Fig. S3. TPD plots of (a) acidic and (b) basic sites in Zn-SDC MOF.

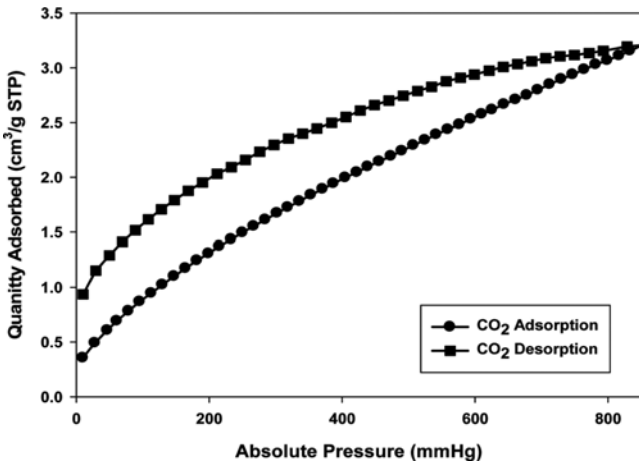

Fig. S4. CO_2 adsorption and desorption for Zn-SDC.

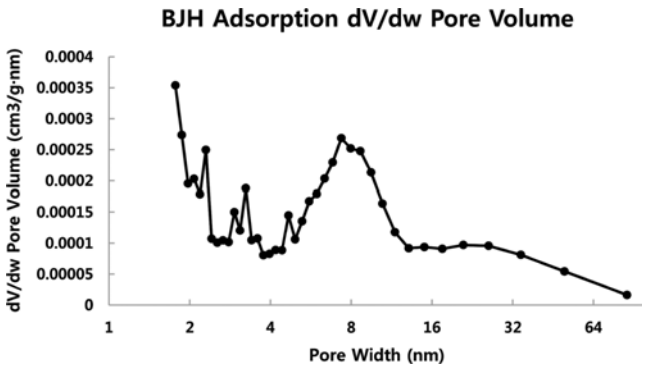

Fig. S5. Pore size distribution of Zn-SDC.

Table S1. Elemental analysis and ICP-OES of Zn-SDC

Zn-SDC	C (wt%)	H (wt%)	O (wt%)	N (wt%)	Zn (wt%)
Calculated	56.83	3.89	19.63	2.46	17.19
Synthesized	57.33	4.21	26.24	2.72	16.65